CHOLESTEROL UPTAKE/TRAFFICKING, STEROID BIOSYNTHESIS AND GONADOTROPIN RESPONSIVENESS ARE DEFECTIVE IN YOUNG WOMEN WITH POOR OVARIAN RESPONSE

PhD program in Reproductive Medicine

Thesis

by Kayhan Yakin, M.D.[1,2]

Advisor:

Özgür Öktem, M.D.[1,2]

[1]Graduate School of Health Sciences, Koç University

[2]Department of Obstetrics and Gynecology, Koç University School of Medicine, Istanbul.

Summary

Poor ovarian response to stimulation is one of the most challenging conditions for clinicians that substantially decreases in-vitro fertilization (IVF) success rates. It is characterized suboptimal or even failed ovarian response to gonadotropin stimulation, lower oocyte yield and live birth rates. It largely remains to be answered as to whether poor response in young IVF patients is simply fewer follicle growth due to diminished ovarian reserve, or there are specific intrinsic perturbations in the functions of the granulosa cells (GCs). The purpose of this study was to analyze and compare steroidogenic function and gonadotropin responsiveness of luteal GCs obtained from poor versus normal responding IVF patients under age 35. The study group comprised 20 women who were diagnosed as poo responders based on a collection of ≤ 3 oocytes in the current ovarian stimulation cycle and an abnormal ovarian reserve test (antral follicle count< 5; anti-Mullerian hormone ≤ 1.2 ng/mL). The control group included 20 women with normal ovarian response. Gonadotropin hormone (GnRH) antagonist and recombinant follicle stimulating hormone (FSH) were used for ovarian stimulation. Luteal GC were obtained during oocyte retrieval procedure, processed and analyzed separately for each individual patient. The expression of steroidogenic enzymes steroidogenic acute regulatory protein (StAR), 3β-hydroxy steroid dehydrogenase (3β-HSD), aromatase, FSH, luteinizing hormone (LH) and low-density lipoprotein (LDL) receptor expression were analyzed by quantitative real-time polymerase chain reaction (qRT-PCR) and immunoblotting methods. The signal intensity of the steroidogenic enzymes and their co-localization with mitochondria and intracellular lipids were assessed using laser confocal immunofluorescence microscopy. The uptake of fluorescent tagged cholesterol and its co-localization with mitochondria were analyzed using time lapse confocal live cell images to monitor cholesterol trafficking in the cells. In vitro estradiol ($E_{2)}$ and progesterone ($P_{4)}$ productions were measured with ECLIA method. Continuous data were compared using ANOVA and multiple comparison post-hoc

tests. While the mean ages of the patients were comparable between two groups, E_2 and P_4 levels at the time of ovulation trigger, mature oocyte yield and clinical pregnancy rates were significantly lower in the poor responders compared to the normal responders. The steroidogenic enzymes, FSH and LH receptors were expressed at significantly lower levels in the GCs of the poor responders in the qRT-PCR and immunoblot analyses. In-vitro E_2 and P_4 production of the GCs of the poor responders were significantly lower than those of the normal responders. Furthermore, these cells poorly responded to exogenously administered FSH and human chorionic gonadotropin (hCG). Confocal imaging showed that the GCs of the poor responders have weaker signal intensities of the steroidogenic enzymes, reduced mitochondrial content, smaller intracytoplasmic lipid accumulation defective co-localization of the mitochondria with steroidogenic enzymes and lipids compared to the normal responders. Furthermore, confocal time-lapse live cell imaging revealed that the uptake of cholesterol and its cytoplasmic accumulation, transportation, and eventual co-localization with mitochondria were significantly delayed and reduced in the poor responders. The expression of LDL receptor was also reduced in the poor responders in the immunoblot analysis and confocal images. Taken together, these findings demonstrate intrinsic defects in the LDL receptor expression, uptake/trafficking of cholesterol, gonadotropin receptor expression, and basal and gonadotropin-stimulated steroidogenesis in the GCs of young poor ovarian responders. From the clinical perspective, poor ovarian response in young individuals should not simply be regarded as fewer follicle growth due to diminished ovarian reserve and the underlying pathogenetic mechanisms appear to be more complex. It is likely that observed defects in steroidogenesis and gonadotropin responsiveness impair not only luteal function but also follicular phase growth characteristics of the poor responders. Further, these defects in the function of luteal GCs of the poor responders also raise an important question of whether they reduce IVF success rate when fresh embryo transfer is contemplated.

INTRODUCTION

Poor ovarian response (POR) to stimulation is a major challenge in assisted reproduction and it is characterized by suboptimal response to gonadotropin stimulation, fewer follicle growth, lower estradiol (E_2) levels, and oocyte yield and poorer live birth rates. The definition of poor responders is vague and the patient population is heterogeneous. As such, 41 different definitions have been used to define the patients with poor ovarian response according to a systematic review of 47 randomized studies (Polyzos and Devroey 2011). In order to reduce heterogeneity the European Society for Human Reproduction and Embryology (ESHRE) introduced the Bologna criteria to define the poor responders (Ferraretti *et al.* 2011). According to these criteria at least two of the following three features must be present in order to define the poor response in IVF: 1) advanced maternal age (≥40 years) or any other risk factor for POR; 2) a previous POR (≤3 oocytes with a conventional stimulation protocol); 3) an abnormal ovarian reserve test based on antral follicle count (AFC) < 5–7 follicles or anti-Mullerian hormone (AMH) <0.5 –1.1 ng/ml. Also, two episodes of POR after maximal stimulation are sufficient to define a patient as a poor responder in the absence of advanced maternal age or abnormal ORT (Ferraretti et al. 2011). The Bologna criteria was criticized by some on the grounds that it did not take into account the oocyte quality and clearly define the risk factors that can be associated with the development of the poor response. Later on, the POSEIDON criteria have been introduced to overcome the shortcomings of the Bologna criteria and allow a better stratification of the poor prognosis patients (Poseidon *et al.* 2016). It suggests four distinct subgroups based on 1) quantitative and qualitative parameters such as age and the expected aneuploidy rate; 2) ovarian reserve biomarkers (AFC and/or AMH); and 3) ovarian response. Group 1: Patients < 35 years with sufficient pre-stimulation ovarian reserve parameters (AFC ≥5, AMH ≥1.2 ng/mL), Group 2: Patients ≥35 years with sufficient pre-stimulation ovarian reserve parameters (AFC≥5, AMH ≥1.2 ng/mL), Group 3: Patients < 35

years with poor ovarian reserve pre-stimulation parameters (AFC <5, AMH <1.2 ng/mL), Group 4: Patients ≥ 35 years with poor ovarian reserve pre-stimulation parameters (AFC <5, AMH <1.2 ng/mL) (Poseidon et al. 2016). Two main categories appear according to this classification system, namely the "expected" (groups 3 and 4) and the "unexpected" PORs (groups 1 and 2) (Poseidon et al. 2016).

Our motivation in designing and conducting this study was to address one fundamental question of whether poor ovarian response in young IVF patients under age 35 with low ovarian reserve is simply a state of fewer follicle growth as a result of diminished ovarian reserve or there are subtle intrinsic defects in gonadotropin responsiveness and steroidogenesis as the underlying molecular pathogenetic mechanism. Unfortunately, this question is yet to be answered and most of the published studies so far investigated the molecular aberrations in a heterogenous population of patient with diminished ovarian reserve (DOR); advanced age or elevated FSH level rather than documented poor responding IVF patients (Seifer *et al.* 1996; Chin *et al.* 2002; May-Panloup *et al.* 2005; Greenseid *et al.* 2011; Skiadas *et al.* 2012; Boucret *et al.* 2015; Shaw *et al.* 2015; Morin *et al.* 2018; Fan *et al.* 2019; Olsen *et al.* 2020; Olsen *et al.* 2021). Therefore, our study population consisted of ≤ 35-year-old normal and poor responding IVF patients. Index control group had good ovarian reserve biomarkers (AFC ≥5, AMH ≥1.2 ng/mL) who underwent ovarian stimulation for different non-ovarian factor infertility etiologies. The poor responders were identified with documentation of both (1) ≤3 oocytes in the current IVF cycles in which the luteal GCs were harvested and used for the experiments, and (2) abnormal ovarian reserve test (AFC<5 and AMH: <1.2 ng/ml) preceding that IVF attempt.

In order to address the study question, a translational research study was designed that entails several different experimental methodologies as illustrated in Figure-1 in which the molecular characteristics of the different steps of steroidogenesis and gonadotropin response were analyzed in the luteal GCs of normal and poor responders.

Figure. 1. Illustration of the experimental methodologies used in the study

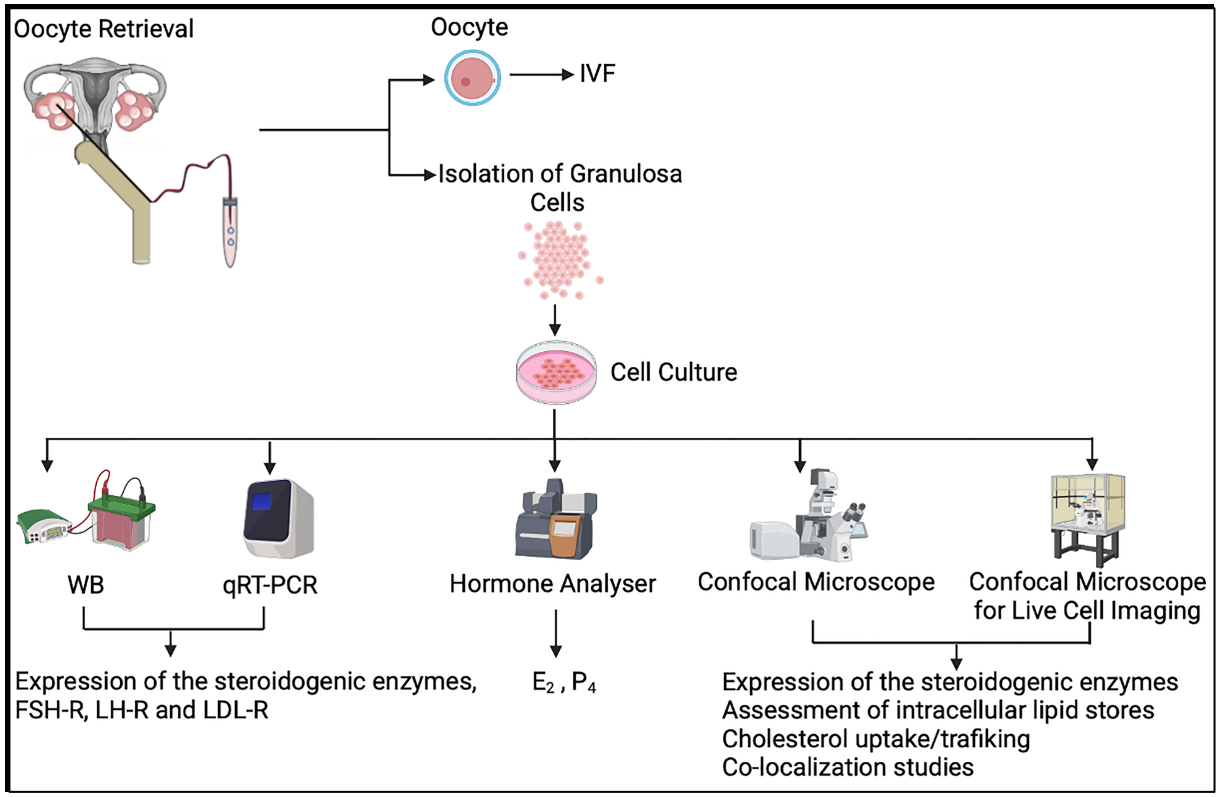

MATERIAL AND METHODS

This study was approved by the Institutional Review Board of Koç University (IRB#2019.299.IRB2.092)

Patients

Forty IVF patients undergoing ovarian stimulation with antagonist protocols using GnRH antagonist (Cetrorelix acetate, Cetrotide, Merck Serono, Germany) and rec FSH (Gonal-F, Merck Serono, Germany) were included in the study. 20 of these patients were normal responders while the remaining 20 were documented poor responders who fulfill the criteria of both Bologna and POSEIDON based on the collection of ≤ 3 oocytes in the current IVF cycle and an abnormal ovarian reserve test (AFC<5, AMH < 1.2 ng/mL) (Ferraretti et al. 2011; Poseidon et al. 2016). Oocyte retrieval was performed 36 hours after ovulation trigger. Recovered luteal GC were processed and analyzed separately for each individual patient. All patients underwent fresh embryo transfers. All eligible IVF patients were invited to participate in this study over a 12-month period between May 2020 and May 2021 until the required sample numbers determined by power analysis calculations were reached. Normal and poor responders with ovarian pathology and/or infertility etiologies (ovarian surgery, cysts, endometriosis etc.) and high responders were excluded from the study in order to reduce the risk of confounding effect of infertility etiology-related factors on the parameters investigated. The patients with metabolic/endocrine disorders, chronic and/or inflammatory systemic diseases, auto-immune disorders, malignancies, previous exposure to radiation and chemotherapy drugs and previous ovarian surgery were also excluded from the study for the same reason.

Isolation and culture of human luteal granulosa cells

Luteal granulosa cells were obtained from follicular aspirates during oocyte retrieval procedure and cultured individually for each patient without pooling as described previously (Bildik *et al.* 2019; Bildik *et al.* 2020). In brief, recovered cells were cultured in 6-well format culture plates at a density of 100,000 cells per well using DMEM-F12 culture medium supplemented with 10% fetal bovine serum at 37°C and 5% CO_2.

Chemicals and reagents

All cell culture materials were obtained from Gibco Inc. Hoechst 33342 (#4082). All western blotting buffers and reagents were purchased from Bio-Rad. Anti-Vinculin Antibody (V9264) was purchased from Sigma-Aldrich. Mouse anti-human monoclonal antibodies were purchased from Santa Cruz Biotechnology for the detection of human 3β-HSD Type II (sc-100466) and StAR (sc-166821). Aromatase (CYP19A, ab34193) monoclonal mouse antibody was from Abcam Inc. Super Block reagent (#AAA125) was purchased from ScyTek Laboratories.

Gene expression analysis

RNA isolation was performed with Quick-RNA MicroPrep Kit (Zymo Research, Irvine, CA, USA) according to the manufacturer's instructions. RNA was quantified with a spectrophotometric read at 260 nm by Nanodrop 2000 (Thermo Fisher Scientific, MA, USA) and 500 ng cDNA was prepared by using M-MLV Reverse Transcriptase (Invitrogen). Quantitative real-time expressions of mRNAs of interest were detected and compared by using Light Cycler 480 SYBR Green I Master (Roche, Germany). The primers of the genes used in the study are listed in Table 1. The means and SDs were calculated from three different readouts taken for each target gene in the RT-PCR assay. ΔΔCt method was used for relative

quantitation of target genes (Livak and Schmittgen 2001; Oktem *et al.* 2017; Bildik et al. 2019; Bildik et al. 2020).

Table 1. The primers of the genes used in the study

Gene		**3'-Sequence-5'**
GAPDH	Forward	ATGGAAATCCCATCACCATCTT
	Reverse	CGCCCCACTTGATTTTGG
StAR	Forward	AAACTTACGTGGCTACTCAGCATC
	Reverse	GACCTGGTTGATGATGCTCTTG
3β-HSD	Forward	GCCTTCAGACCAGAATTGAGAGA
	Reverse	TCCTTCAAGTACAGTCAGCTTGGT
Aromatase	Forward	GGTCACCACGTTTCTCTGCT
	Reverse	GCAAGCTCTCCTCATCAAACCA
LH-R	Forward	TTGAACTGAGGTTTGTCCTCACCA
	Reverse	GGCCTCAGGGTTGATGTAGAGC
FSH-R	Forward	TTTCAAGAACAAGGATCCATTCC
	Reverse	CCTGGCCCTCAGCTTCTTAA

Immunoblotting

The 3β-hydroxysteroid dehydrogenase (3β-HSD) Type II (sc-100466) and (Steroidogenic acute regulatory protein (StAR) (sc-166821) monoclonal antibodies were purchased from Santa Cruz Biotechnology (Santa Cruz Biotechnology, Inc., TX, USA). Aromatase (CYP19A, ab34193) monoclonal mouse antibody was from Abcam (Abcam Inc., MA, USA). LDL receptor polyclonal antibody was purchased from Cayman Chemicals (Item no.10007665, Cayman Chemicals, USA). Anti-vinculin antibody (Sigma-Aldrich, St. Louis, MO, USA) was used as loading control at a dilution of 1:10,000. Cell lysates for western blot were prepared using radioimmunoprecipitation assay buffer (Sigma-Aldrich) as described previously (Oktem et al. 2017). Immun-Blot® PVDF Membranes (BioRad, CA, USA) were incubated overnight at 4°C with the antibodies at the concentrations recommended by the manufacturers.

Conventional and Confocal Laser Immunofluorescence Imaging

Cells were fixed in 4% PFA for 30 min at RT, washed twice with PBS and permeabilized (except for LDL-R) with 0.1% Triton-X100 in DPBS for 8 min. Blocking was performed with Superblock for 10 min. Steroidogenic enzymes (StAR and 3B-HSD), LDL-R and mitochondria (mitotracker) were detected using immunofluorescence staining method as described previously (Bildik *et al.* 2020). The images were taken under appropriate channels using a confocal microscope (Leica, DMI8). Oil Red O (Sigma, USA) as a fat-soluble dye is used for staining of natural triglycerides and lipid droplets of the cells. Oil Red O working solution (0.5%) was prepared by boiling of 0.5 g Oil Red O in 100 ml 100% isopropanol. Cells were washed with Dulbecco's phosphate-buffered saline (DPBS) and fixed with 4% paraformaldehyde (PFA) for 20 min at RT. Following washing with DPBS, cells rinsed at 60% isopropanol and stained with Oil Red O (Sigma, USA) for 20 min at RT. Subsequently, cells were rinsed by 60% isopropanol and running tap water respectively and prepared for immunofluorescence staining steps. Permeabilization was performed (if necessary) in 0.2% Triton X-100 containing DPBS for 20 min at RT. Blocking of nonspecific epitopes was performed by incubation in Super Block (ScyTek, USA) medium for 20 min at RT. Thereafter, the cells were incubated with primary antibodies for overnight at 4 °C. Cells were washed three times with DPBS-Tween (0.01%), then incubated with secondary antibodies for 1 h at 37 °C. Cells were washed three times, then covered with Fluoroshield mounting medium with DAPI (Abcam, UK) and images were taken using a confocal microscope (Leica, DMI8).

Confocal Live Cell Imaging for Cholesterol Uptake/Trafficking

For timeline visualizing of cholesterol uptake process and mitochondria, cells were stained lively using NBD-Cholesterol (Invitrogen) and Mitotracker (Invitrogen), respectively. Briefly, cells were cultured in glass bottom dishes (Thermofisher) a day before staining. The day after,

medium was replaced by 1 ml fresh medium, which contains NBD-Cholesterol (1 μg/ml), Mitotracker (100 nM) and Hoechst (1 μg/ml). Subsequently, cells were transferred into confocal microscopy (Leica, DMI8) equipped with an incubation chamber (37 °C, 5% CO_2) for live cell imaging. Previous in vitro and in vivo findings demonstrated NBD-cholesterol to be useful as a fluorescent probe for real-time imaging of lipoprotein-mediated cholesterol uptake and trafficking (Huang *et al.* 2015).

Hormone assays

E_2 and P_4 levels in culture media were determined by using electrochemiluminescence immunoassay "ECLIA" (Elecsys and Cobas immunoassay analyzers, Roche Diagnostics, USA). Lower detection limits of E2 and P were 5.00 pg/ml (18.4 pmol/ml) and 0.030 ng/ml (0.095 nmol/ml), respectively.

Statistical analysis

Samples size required for statistical significance and proper interpretation of the results were calculated based on the qRT-PCR assays and immunoblot assays. The mean and standard deviation (SD) values were calculated from three different readouts taken for each target gene in the RT-PCR assay. mRNA levels of the target genes used in the qRT-PCR assay (steroidogenic enzymes, FSH/LH receptor) and hormone levels are continuous variables therefore, expressed as the mean±SD. ANOVA/ Bonferroni or Kruskal Wallis/Dunn post hoc tests were applied to compare the groups if data are parametric or non-parametric respectively. Paired t-test was applied to compare the signal intensity of the steroidogenic enzymes and hormone levels before and after FSH and hCG treatments. Significance level was set at 5% ($P < 0.05$) and the Graphpad Prism version 9 was used to analyze the data and create the figures.

RESULTS

Clinical characteristics and outcomes of the IVF cycles

Demographic and IVF cycle characteristics of the patients are summarized in Table II. The IVF cycles were comparable in terms of age, gonadotropin dose and duration of stimulation. Serum E_2 and P_4 levels on the day of ovulation trigger, the number of oocytes retrieved and clinical pregnancy rates were significantly lower in the poor responders compared to the normal responders. Comparison of molecular characteristics of the steroidogenic function of the GCs of normal and poor responders were carried out using several different experimental methodologies as illustrated in Figure 1.

Basal and gonadotropin-stimulated steroidogenesis and gonadotropin response are defective in the poor responders

Comparison of mRNA expression of steroidogenic enzymes and gonadotropin receptors in qRT-PCR showed significantly lower levels of the transcripts of StAR, 3β-HSD, aromatase, and FSH and LH receptors in the GCs of the poor responders compared to the normal responders (Figure-2A). Consistent with the qRT-PCR results, immunoblot analysis showed that the expression of StAR, 3β-HSD and aromatase were significantly reduced in the poor responders than the normal responders (Figure-2B and 2C).

Comparison of the in-vitro steroidogenic activity of the cells revealed that when plated at equal density, the GCs of poor responders produced significantly lower amounts of E_2 (628.8±160 vs. 1017±176 pg/mL respectively, $p<0.0001$) and P_4 (382±128 vs. 690±119 ng/mL respectively, $p<0.0001$) after 24h culture period in comparison to normal responders (Figure-2D).

Table II. Demographic and cycle characteristics of the patients

	Normal responder	Poor responder
N	20	20
Female age (y)	32.2 ± 1.8 (30-35)	33.0 ± 1.8 (30-35)
Male age (y)	34.8 ± 4.3 (29-43)	35.2 ± 4.5 (30-42)
Duration of infertility (y)	2.5 ± 2.3 (1-4)	2.7 ± 1.7 (1-4)
BMI (kg/m^2)	24.5±2.6 (20.4-31.2)	24.8±2.5 (20.8-29.1)
Duration of stimulation (d)	10.5±1.3 (8-13)	10.1±2.0 (8-15)
Initial gonadotropin dose (IU)	266±38 (225-300)[a]	322±54 (300-450)
AMH (ng/dl)	2.1±0.6 (1.73-2.81)[a]	0.67±0.33 (0.07-1.08)
hCG day E2 (pg/dl)	3009.7±564.0 (1264-3422)[a]	936.6±194.3 (398-1241)
hCG day P4 (ng/dl)	0.60±0.39 (0.08-1.41)[b]	0.28±0.15 (0.01-0.92)[b]
No. >14 mm follicles	8.3±2.6 (4-14)[a]	2.1±0.9 (1-3)
Leading follicle (mm)	20.3±1.3 (18.0-22.0)	19.2±1.0 (18.0-21.5)
Endometrial thickness (mm)	10.2±2.6 (7-17)	9.5±1.7 (7-12.9)
No. total oocytes	10.2±2.7 (8-15)[a]	2.6±0.4 (1-3)
No. MII oocytes	8.6±2.3 (8-12)[a]	2.2±0.2 (1-3)
No. 2PN	7.3±2.0 (4-14)[a]	1.2±0.6 (1-3)
No. transferred embryos	1.3±0.5 (1-2)	1.5±0.5 (1-2)
Pregnancy (%)	15/20 (75%)[b]	5/20 (25%)

Values are represented as mean ± SD (range) or number (percentage)
a: $p<0.0001$ b: $p<0.001$

Figure-2: Comparison of the steroidogenic function of the luteal granulosa cells between normal versus poor responders using gene expression studies with qRT-PCR and immunoblotting.

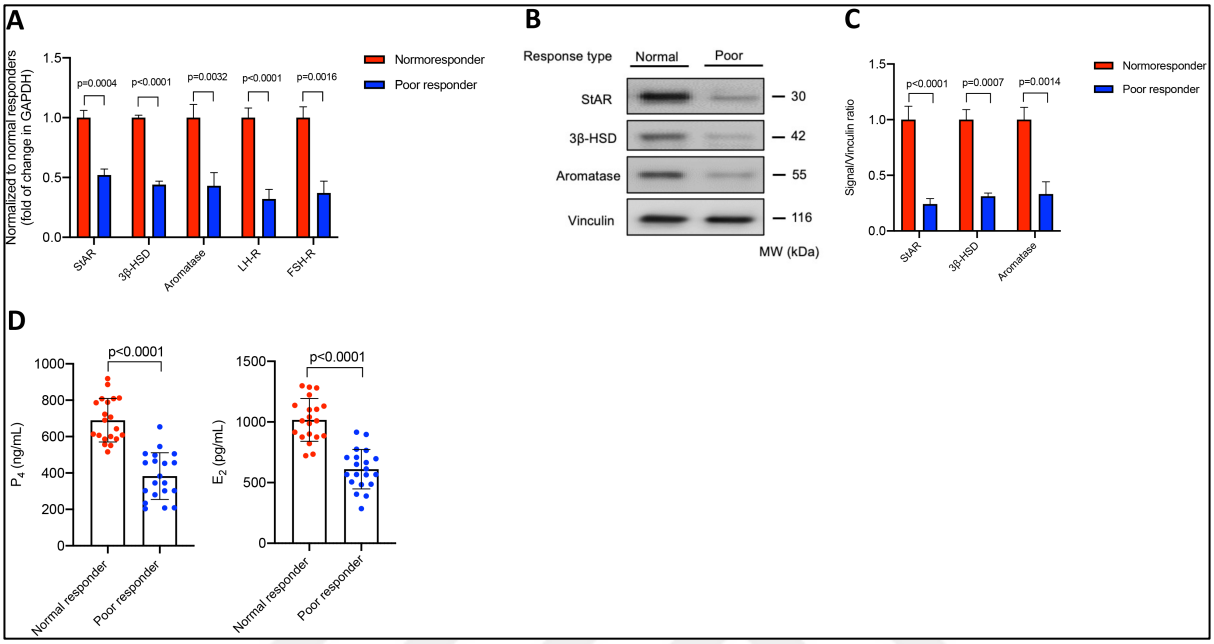

The expression of the steroidogenic enzymes and gonadotropin receptors are significantly down-regulated in the poor responders in the qRT-PCR (2A) and immunoblotting images (2B) and after quantitative comparison of the signals of the immunoblotting (2C). Steroidogenic capacity of the cells is compared by measuring their 24h progesterone (P_4) and estradiol (E_2) output (2D) in-vitro. P_4 and E_2 production are substantially compromised in the poor responders. StAR: Steroidogenic acute regulatory protein, 3β-HSD: 3-beta hydroxy steroid dehydrogenase, LH-R: Luteinizing hormone receptor; FSH-R: Follicle stimulating hormone receptor.

Defective expression of FSH and LH receptors in the GCs of poor responders on qRT-PCR analysis led us to analyze the gonadotropin responsiveness of these receptors. For this purpose, the GCs were treated with rec- hCG and rec-FSH and compared the increase in StAR expression and E_2 and P_4 output between normal versus poor responders. The increases in the expression of StAR and P_4 output were lesser after hCG treatment in the poor responders compared to the normal responders (Figure-3A, 3B and 3C). A similar blunted response was observed after FSH stimulation. The up-regulation in StAR expression and E_2 output were significantly lower in the poor responders (Figure-3D, 3E and 3F).

Figure-3: Comparative analysis of the response of the gonadotropin receptors to exogenous FSH and hCG in the luteal granulosa cells in normal versus poor responders.

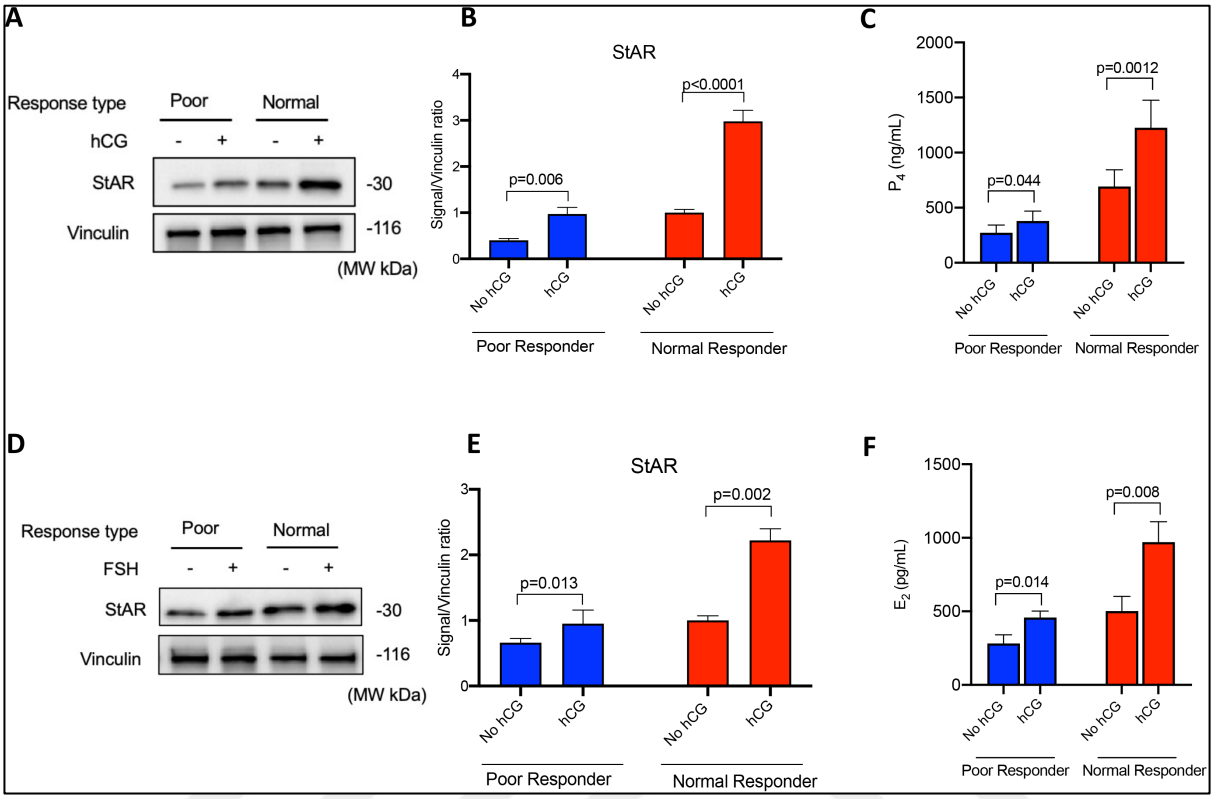

LH receptor responsiveness is assessed by comparing the increase in StAR expression (3A and 3B) and P_4 output (3C) after treatment with hCG. FSH receptor responsiveness was analyzed in a similar fashion by analyzing StAR expression pattern (3D and 3E) and E_2 output (3F) following FSH treatment. Note the more robust increase in the expression of StAR and E_2 and P_4 production after gonadotropin stimulation in the normal responders in comparison to the poor responders.

Taken together these findings so far indicate that i) the expression of the steroidogenic enzymes and gonadotropin receptors are defective; ii) basal and gonadotropin-stimulated steroidogenesis are impaired in the GCs of the poor responders.

Conventional and laser confocal immunofluorescence imaging

Conventional immunofluorescence microscopy examination showed significantly diminished cytoplasmic accumulation of intracellular lipids as assessed by Oil Red O staining in the luteal GCs of the poor responders compared to the normal responders (Figure-4A and 4B). A more detailed analysis with confocal microscopy confirmed this finding (Figure-4C) and also

revealed that mitochondrial content (Figure-4D) as evidenced by weaker signal intensity of mitotracker, and mitotracker/Oil Red co-localization, the indicator of lipid content within the mitochondria (Figure-4E) significantly reduced in the GCs of the poor responders in comparison to the normal responders.

Figure-4: Conventional and confocal microscopic images of lipid stores and mitochondria in the granulosa cells of normal versus poor responders.

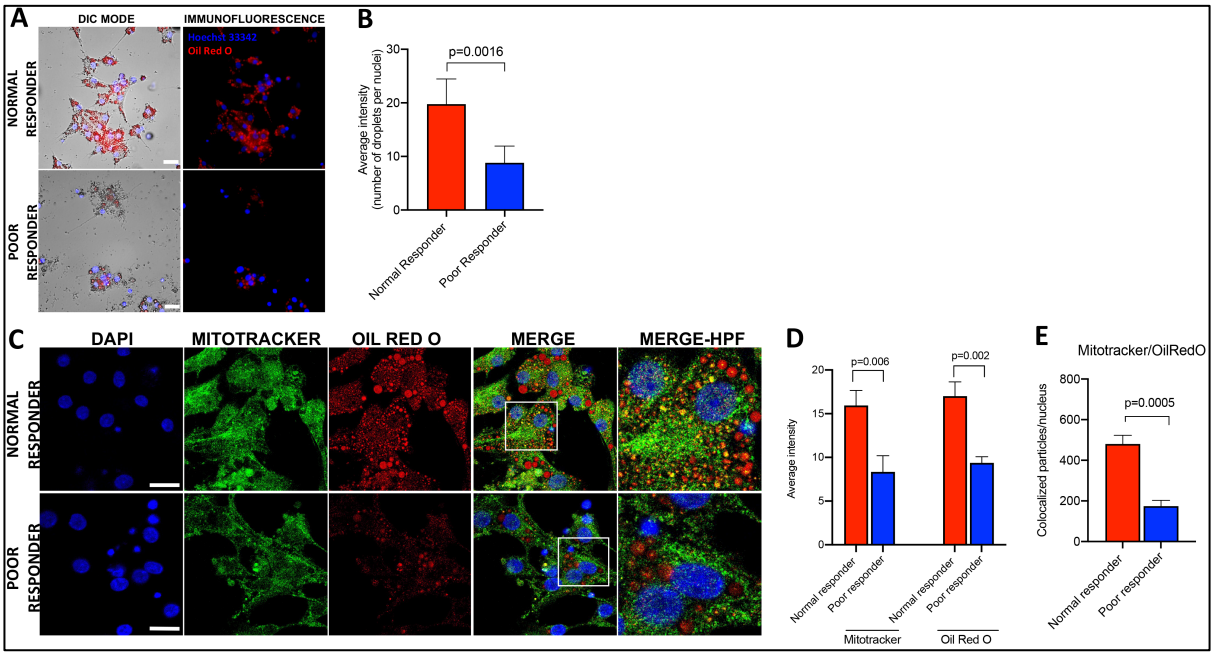

Cytoplasmic lipids and mitochondria are assessed after staining with Oil Red O and fluorescent mitochondrial marker mitotracker respectively, under conventional (4A and 4B) and confocal microscopy (4C to 4E). Mitotracker (green signal) and Oil Red staining (red signal) and their co-localization (yellow signal in merge images) in the confocal image (4C). Their intensity (4D) and co-localization (4E) are shown as graphic bars. Note the weaker signal intensity of mitotracker and Oil Red indicative of less mitochondrial content and lipid accumulation respectively, and the paucity of yellow signals in the poor responders. The areas marked as white squares in the merge images are also shown as high magnification merge images (merge HPF) . Scale bars 25 µ. DAPI (blue signals) are fluorescent nuclear stains.

Consistent with reduced expression of the steroidogenic enzymes in immunoblotting in the poor responders, the signal intensities of StAR (Figures 5A and 5B) and 3β-HSD (Figures 5D and 5E) significantly diminished and their co-localizations with mitochondria (Figures 5C and 5F) markedly reduced in the poor responders when compared to the normal responders.

Figure-5: Confocal images of steroidogenic enzymes and mitochondria in the granulosa cells of the normal and poor responders.

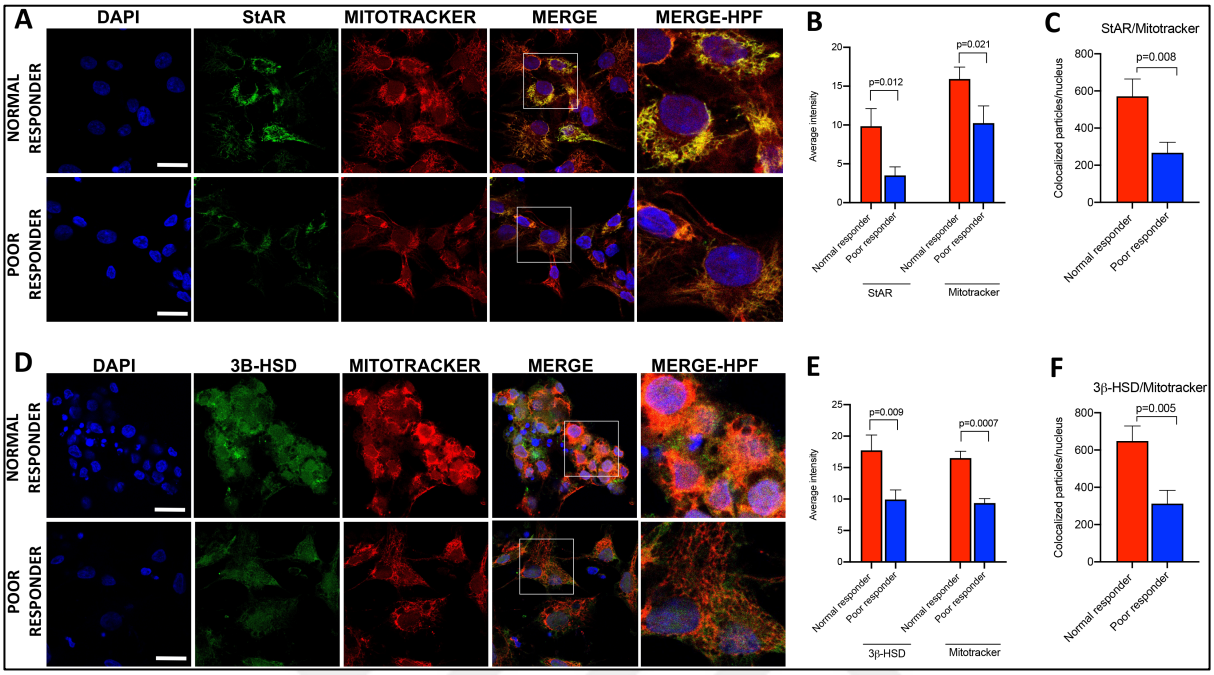

The signal intensity of StAR (green signal) and mitotracker (red signal) and their co-localization (yellow signals in the merge images) are significantly diminished in the poor responders (5A and 5B). Note the paucity of the yellow signals, indicative of the presence of less StAR enzyme within the mitochondria in the merge and HPF merge images. The co-localization is also expressed as a graphic bar (5C). A similar staining pattern is observed for 3β-HSD and mitotracker (5D-5F). The areas marked as white squares are also depicted as high magnification merge image. The areas marked as white squares in the merge images are also shown as high magnification merge images (merge HPF) . Scale bars 25 µ. DAPI (blue signals) are fluorescent nuclear stains.

Monitoring and assessment of intracellular lipids and cholesterol trafficking in the luteal granulosa cells via confocal real-time live cell microscopy

The uptake of NBD cholesterol was monitored using confocal real-time live cell imaging. There was a substantial delay and reduction in its uptake, cytoplasmic accumulation and transportation to mitochondria in the poor responders. Mitotracker/NBD cholesterol co-localization was markedly diminished in the poor responders (Figure-6A to 6D and Movies-1 to 4). LDL-R expressed in the plasma membrane of the steroidogenic cells are primarily responsible for cholesterol uptake.

Figure-6: NBD Cholesterol uptake assay with time lapse live imaging in confocal microscopy

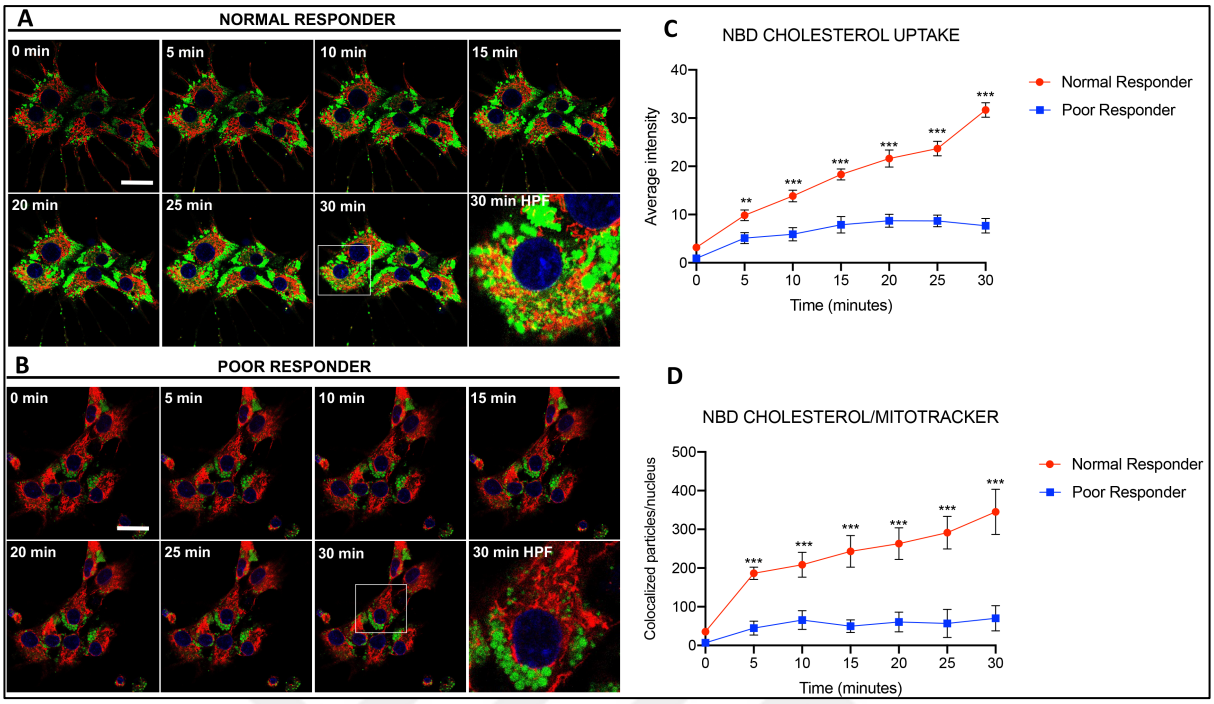

Green fluorescent cholesterol analog NBD cholesterol is rapidly up-taken by the luteal granulosa cells (GCS) in the normal responders and begins to accumulate in their cytoplasm within 30 min after its administration as evidenced by a rapid and steady increase in the intensity of the green signal in the cytoplasm of the cells (6A) and after quantification of the signals as a graphic bar (6C). At the end of the monitoring period its transportation to mitochondria (red signal) is easily identified as strong yellow signals (6A-HPF). The NBD cholesterol/mitotracker lo-localization is also shown as a curve as co-localized particles in the graphic bar. By contrast, such a drastic uptake and co-localization are not observed in the poor responders (6B and 6D). Scale bars 25 µ. Hoechst (blue signals) are fluorescent nuclear stains. Comparison is statistically significant at the level $p<0.001$ (**) and $p<0.0001$ (***).

As the last set of experiments, LDL receptor expression was assessed using immunoblotting and confocal microscopy. LDL-R expression in the luteal GCs of the poor responders was significantly reduced when compared to the GCs of the normal responders (Figure-7A to 7E).

Figure-7: Confocal images of the granulosa cells stained for the analysis of LDL receptor and lipids stores.

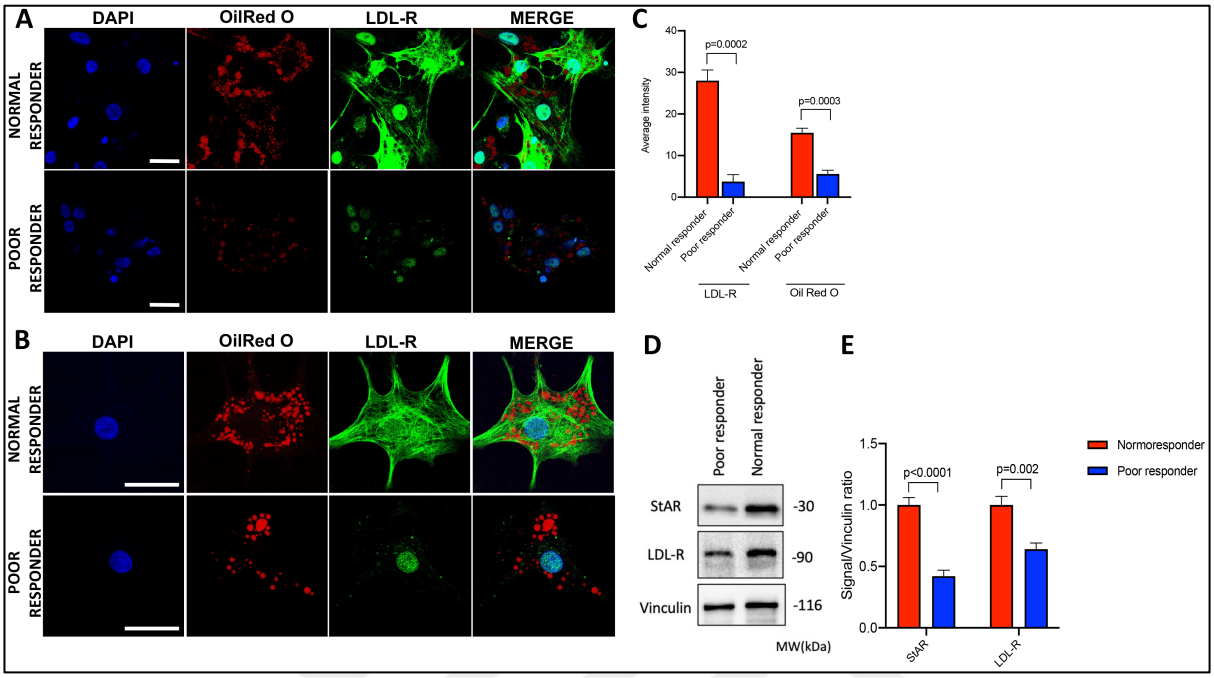

The signal intensity of LDL-R (green signal) is much weaker and intracytoplasmic lipid accumulation as assessed by Oil Red O staining (red signal) are significantly reduced in the luteal granulosa cells (GCs) of the poor responders (7A to 7C). Similarly, the expression of LDL-R was significantly diminished along with StAR in the poor responders in the immunoblot images (7D) and depicted as graphic bar after quantitative comparison of the immunoblot signals (7E). Scale bars 25 µ. DAPI (blue signals) are fluorescent nuclear stains.

DISCUSSION

This study analyzes several steps of steroid biosynthesis in luteal GCs and showed several intrinsic defects in the steroidogenic pathway in the young poor responding IVF patients as follows: (1) Reduced expression of the steroidogenic enzymes (StAR, 3β-HSD and aromatase) and gonadotropin receptors, (2) Impaired steroidogenic response to FSH and hCG, (3) Defective basal and gonadotropin-stimulated E_2 and P_4 productions, (4) Reduced mitochondrial content and defects in its co-localizations with steroidogenic enzymes and lipids, (5) Reduced LDL receptor expression, impaired cholesterol uptake and its intracellular trafficking, and intracytoplasmic accumulation.

From the clinical perspective, the findings of this research indicate that POR to stimulation should not simply be considered as a state of fewer follicle growth or oocyte yield due to DOR and that the underlying molecular perturbations leading to POR are much more complex, involving multiple steps in steroidogenesis and gonadotropin responsiveness.

Steroidogenesis entails a multi-step physiological process in which cholesterol is converted into steroid hormones. In brief, steroidogenic cells take up circulating cholesterol mainly in the form of LDL via LDL receptor-mediated endocytosis and then direct cholesterol for steroid hormone synthesis to mitochondria or stored in lipid droplets after esterification. StAR is the rate limiting enzyme of steroid biosynthesis and facilitates the rapid flux of free (unesterified) cholesterol into mitochondria in steroidogenic cells. While 3β-HSD catalyzes the conversion of Δ^5 steroids to the corresponding Δ^4 steroids including the conversion of pregnenolone to progesterone within the mitochondria aromatase (CYPA1) as a CYP450 enzyme catalyzes the conversion of androgens to estrogens (Miller 2017).

To date, a limited number of studies have analyzed the steroidogenic characteristics of the luteal GCs obtained from a heterogenous population of patients with DOR, advanced age and POR. Thus, the existing data is still limited and somewhat inconsistent for and methodological/technical limitations as none has carried out a detailed comparative analysis of different steps of steroidogenesis. Seifer et al compared E_2 and P_4 production of the luteal GCs between seven women with low day 3 FSH (≤6IU/mL) versus. 8 women with high day 3 FSH (≥10IU/mL) and did not observe any difference in the steroidogenic activity between the groups. The sample size was low and the number of oocytes retrieved was within the normal range even in the high FSH group (8.6±1.3), raising the question of whether these patients were real poor responders (Seifer et al. 1996). Later on, several studies compared the viability of luteal GCs between normal younger versus. poor older responders with inconsistent results (Chin et al. 2002; Muhammad *et al.* 2009; Greenseid et al. 2011; Fan et al. 2019). Reactive oxygen species and mitochondrial DNA content play critical roles in cellular ageing (Park *et al.* 2021). In this regard, Tatone et al demonstrated in luteal GCs that the mean relative levels of mRNAs coding for superoxide dismutases, Cu, ZnSOD (SOD1), MnSOD (SOD2) and catalase were significantly decreased in women older than age 38 years. Similar to our findings, the authors also observed that the GCs of older women (range 38-41 years) showed defective mitochondria and fewer lipid droplets than those observed in the younger group (range 27-32 years) and attributed those findings in older patients to age-dependent oxidative stress injury (Tatone *et al.* 2006). In addition to this study several other groups demonstrated reduced mitochondrial DNA content in the oocytes and cumulus GCs of the older IVF patients with DOR and ovarian insufficiency (May-Panloup et al. 2005; Duran *et al.* 2011; Boucret et al. 2015; May-Panloup *et al.* 2016).

This study has several limitations. The analyses were performed in a relatively specific patient population. Therefore, it is unclear if the observed defects are universally present in all subtypes of poor response regardless of chronological age and ovarian reserve status and if they vary depending upon infertility etiology. Although advanced age and diminished ovarian reserve are generally the most common etiological factors that explain poor ovarian response to ovarian stimulation, at least some proportions of poor responders are still young (Poseidon et al. 2016), indicating that there must be some other factors that are implicated in the pathophysiology of poor response. Development of poor response to stimulation in young patients with normal ovarian reserve indices further complicates the scene. It is likely that different pathogenetic mechanisms are operative for young versus older poor responders. Advanced maternal age and ageing-related decline in ovarian reserve are associated with a reduction not only in oocyte quantity but also in oocyte quality, and significantly increase the risk of embryo aneuploidy (Cimadomo *et al.* 2018; Mikwar *et al.* 2020). Thus, the prognosis is differentially impacted by female age and ovarian reserve (oocyte quantity) as the former is more closely associated with embryo aneuploidy. However, there is also evidence that links low ovarian reserve, regardless of chronological age, to an increase in oocyte aneuploidies and miscarriage risk (Haadsma *et al.* 2010; Haadsma *et al.* 2010; van der Stroom *et al.* 2011; Sunkara *et al.* 2014), and lower fertilization rates (Lekamge *et al.* 2007), indicative of some intrinsic defects in oocytes that cannot be attributed to ageing.

It is a matter of debate whether premature senescence might play a role in the development of DOR and poor ovarian response to stimulation in young patients? While there is still no universal consensus on the exact definition of premature ageing/senescence and its role on ovarian function/senescence, two recent papers from the same group of investigators were able to show the signs of premature ageing in the GCs and oocytes in young patients with low

ovarian reserve indices (Olsen et al. 2020; Olsen et al. 2021). The investigators compared the luteal GCs between the patients with normal versus diminished ovarian reserve (DOR) via whole-genome methylation array data utilizing DNA methylation variability, age acceleration, DNA methylation telomere length estimator (DNAmTL), and accumulation of epimutations. Their findings demonstrated that luteal GCs of women with DOR have a distinctive epigenetic profile and harbor a high frequency of epimutations suggestive of premature aging, and appear epigenetically more like women with advanced age (>40) (Olsen et al. 2020; Olsen et al. 2021). On the other hand, another interesting study assessed the accuracy of the "epigenetic clock" concept in reproductive age women undergoing fertility treatment by applying the age prediction algorithm in peripheral (white blood cells [WBCs]) and follicular somatic cells (cumulus cells [CCs]) in order to investigate whether women with premature reproductive aging (diminished ovarian reserve) were at risk of accelerated ageing in their age prediction. The study utilized the methylation level of 353 CpG sites from white blood cells (WBC) and cumulus GCs of younger and older IVF patients with normal and poor response and demonstrated that while WBC accurately predicted the chronological age of the patients the cumulus GCs did not. Furthermore, the cumulus GCs were found to have longer telomere lengths than WBCs and the authors observed that categorization of patients according to ovarian response did not appreciably change the age prediction in WBCs or CCs, neither was it associated with relative telomere DNA length (Morin et al. 2018). Taken collectively, it remains elusive if premature ageing develops in the ovary and if any, to what extent it causes reproductive senescence by depleting ovarian reserve and/or impairing gonadotropin response in young poor responders who have low ovarian reserve discordant with their chronological age.

Animal data showed ageing related decline in LH responsiveness, cAMP production and cholesterol transport to mitochondria in rats (Zirkin and Chen 2000; Chen *et al.* 2002; Wang *et al.* 2017). However, no evidence in humans exists yet to link the perturbations in steroidogenesis and gonadotropin response to the detrimental effect of ageing/oxidative stress or another pathological process. This is also true for our findings. On the other hand, there is solid evidence that ovarian steroidogenesis is well preserved in regularly cycling older women and even continues unhampered up until a few years before final cessation of menses despite age-related decline in ovarian reserve, higher FSH, lower inhibin-B and AMH levels (Musey *et al.* 1987; Burger *et al.* 2000; Broekmans *et al.* 2009; Shaw et al. 2015).

Another question is whether the observed perturbations in the steroidogenic function of the luteal GCs of the poor responders contribute to lower IVF success rates when fresh embryo transfer is performed. To date, several observational or retrospective studies compared fresh versus freeze all strategies in the poor responders with inconsistent results (Celik *et al.* 2015; Berkkanoglu *et al.* 2017; Roque *et al.* 2018; Liu *et al.* 2021). In the meantime, the indications of the freeze all strategy such as P_4 elevation on the hCG day, the history of one previously failed fresh cycle as well as the differences in endometrium between fresh and frozen cycles should be taken into the considerations as the possible confounders that may impact upon the IVF success rate while remembering at the same time the very fact that many poor responders do not have the luxury of elective embryo freezing and undergo compulsory fresh embryo transfer cycles.

Conclusion

This study unveils previously unknown intrinsic defects in the steroidogenic function of the granulosa cells of the young poor responder, underscoring the complexity of this phenomenon rather than simply being a state of fewer follicle growth/oocyte yield due to diminished ovarian reserve. Caution should be exercised when interpreting the data as it is unclear if the observed defects exhibit variations according to the race, poor response type, ovarian response type, stimulation protocol, infertility etiology and the mode of ovulation trigger.

References

Berkkanoglu M, Coetzee K, Bulut H and Ozgur K. Optimal embryo transfer strategy in poor response may include freeze-all. J Assist Reprod Genet. 2017; **34**(1): 79-87.

Bildik G, Akin N, Esmaeilian Y, Hela F, Yakin K, Onder T, Urman B and Oktem O. hCG Improves Luteal Function and Promotes Progesterone Output through the Activation of JNK Pathway in the Luteal Granulosa Cells of the Stimulated IVF Cycles. Biol Reprod. 2020; **102**(6): 1270-1280.

Bildik G, Akin N, Esmaeilian Y, Hela F, Yildiz CS, Iltumur E, et al. Terminal differentiation of human granulosa cells as luteinization is reversed by activin-A through silencing of Jnk pathway. Cell Death Discov. 2020; **6**: 93.

Bildik G, Akin N, Seyhan A, Esmaeilian Y, Yakin K, Keles I, et al. Luteal granulosa cells from natural cycles are more capable of maintaining their viability, steroidogenic activity and LH receptor expression than those of stimulated IVF cycles. Hum Reprod. 2019; **34**(2): 345-355.

Boucret L, Chao de la Barca JM, Moriniere C, Desquiret V, Ferre-L'Hotellier V, Descamps P, et al. Relationship between diminished ovarian reserve and mitochondrial biogenesis in cumulus cells. Hum Reprod. 2015; **30**(7): 1653-1664.

Broekmans FJ, Soules MR and Fauser BC. Ovarian aging: mechanisms and clinical consequences. Endocr Rev. 2009; **30**(5): 465-493.

Burger HG, Dudley E, Mamers P, Groome N and Robertson DM. Early follicular phase serum FSH as a function of age: the roles of inhibin B, inhibin A and estradiol. Climacteric. 2000; **3**(1): 17-24.

Celik S, Turgut NE, Yagmur E, Boynukalin K, Celik DC, Findikli N, Purisa S and Bahceci M. The effects of fresh embryo transfers and elective frozen/thawed embryo transfers on

pregancy outcomes in poor ovarian responders as defined by the Bologna criteria. Turk J Obstet Gynecol. 2015; **12**(3): 132-138.

Chen H, Hardy MP and Zirkin BR. Age-related decreases in Leydig cell testosterone production are not restored by exposure to LH in vitro. Endocrinology. 2002; **143**(5): 1637-1642.

Chin KV, Seifer DB, Feng B, Lin Y and Shih WC. DNA microarray analysis of the expression profiles of luteinized granulosa cells as a function of ovarian reserve. Fertil Steril. 2002; **77**(6): 1214-1218.

Cimadomo D, Fabozzi G, Vaiarelli A, Ubaldi N, Ubaldi FM and Rienzi L. Impact of Maternal Age on Oocyte and Embryo Competence. Front Endocrinol (Lausanne). 2018; **9**: 327.

Duran HE, Simsek-Duran F, Oehninger SC, Jones HW, Jr. and Castora FJ. The association of reproductive senescence with mitochondrial quantity, function, and DNA integrity in human oocytes at different stages of maturation. Fertil Steril. 2011; **96**(2): 384-388.

Fan Y, Chang Y, Wei L, Chen J, Li J, Goldsmith S, Silber S and Liang X. Apoptosis of mural granulosa cells is increased in women with diminished ovarian reserve. J Assist Reprod Genet. 2019; **36**(6): 1225-1235.

Ferraretti AP, La Marca A, Fauser BC, Tarlatzis B, Nargund G, Gianaroli L and Definition EwgoPOR. ESHRE consensus on the definition of 'poor response' to ovarian stimulation for in vitro fertilization: the Bologna criteria. Hum Reprod. 2011; **26**(7): 1616-1624.

Greenseid K, Jindal S, Hurwitz J, Santoro N and Pal L. Differential granulosa cell gene expression in young women with diminished ovarian reserve. Reprod Sci. 2011; **18**(9): 892-899.

Haadsma ML, Groen H, Mooij TM, Burger CW, Broekmans FJ, Lambalk CB, Leeuwen FE, Hoek A and Group OP. Miscarriage risk for IVF pregnancies in poor responders to ovarian hyperstimulation. Reprod Biomed Online. 2010; **20**(2): 191-200.

Haadsma ML, Mooij TM, Groen H, Burger CW, Lambalk CB, Broekmans FJ, et al. A reduced size of the ovarian follicle pool is associated with an increased risk of a trisomic pregnancy in IVF-treated women. Hum Reprod. 2010; **25**(2): 552-558.

Huang H, McIntosh AL, Landrock KK, Landrock D, Storey SM, Martin GG, et al. Human FABP1 T94A variant enhances cholesterol uptake. Biochim Biophys Acta. 2015; **1851**(7): 946-955.

Lekamge DN, Barry M, Kolo M, Lane M, Gilchrist RB and Tremellen KP. Anti-Mullerian hormone as a predictor of IVF outcome. Reprod Biomed Online. 2007; **14**(5): 602-610.

Liu C, Li Y, Jiang H, Liu Y and Song X. The clinical outcomes of fresh versus frozen embryos transfer in women >/=40 years with poor ovarian response. Obstet Gynecol Sci. 2021; **64**(3): 284-292.

Livak KJ and Schmittgen TD. Analysis of relative gene expression data using real-time quantitative PCR and the 2(-Delta Delta C(T)) Method. Methods. 2001; **25**(4): 402-408.

May-Panloup P, Boucret L, Chao de la Barca JM, Desquiret-Dumas V, Ferre-L'Hotellier V, Moriniere C, Descamps P, Procaccio V and Reynier P. Ovarian ageing: the role of mitochondria in oocytes and follicles. Hum Reprod Update. 2016; **22**(6): 725-743.

May-Panloup P, Chretien MF, Jacques C, Vasseur C, Malthiery Y and Reynier P. Low oocyte mitochondrial DNA content in ovarian insufficiency. Hum Reprod. 2005; **20**(3): 593-597.

Mikwar M, MacFarlane AJ and Marchetti F. Mechanisms of oocyte aneuploidy associated with advanced maternal age. Mutat Res. 2020; **785**: 108320.

Miller WL. Steroidogenesis: Unanswered Questions. Trends Endocrinol Metab. 2017; **28**(11): 771-793.

Morin SJ, Tao X, Marin D, Zhan Y, Landis J, Bedard J, Scott RT and Seli E. DNA methylation-based age prediction and telomere length in white blood cells and cumulus cells of infertile women with normal or poor response to ovarian stimulation. Aging (Albany NY). 2018; **10**(12): 3761-3773.

Muhammad F, Yivgi-Ohana N, Shveiky D, Orly J, Alexander S and Laufer N. Levels of steroidogenic acute regulatory protein and mitochondrial membrane potential in granulosa cells of older poor-responder women. Fertil Steril. 2009; **91**(1): 220-225.

Musey VC, Collins DC, Musey PI, Martino-Saltzman D and Preedy JR. Age-related changes in the female hormonal environment during reproductive life. Am J Obstet Gynecol. 1987; **157**(2): 312-317.

Oktem O, Akin N, Bildik G, Yakin K, Alper E, Balaban B and Urman B. FSH Stimulation promotes progesterone synthesis and output from human granulosa cells without luteinization. Hum Reprod. 2017; **32**(3): 643-652.

Olsen KW, Castillo-Fernandez J, Chan AC, la Cour Freiesleben N, Zedeler A, Bungum M, et al. Identification of a unique epigenetic profile in women with diminished ovarian reserve. Fertil Steril. 2021; **115**(3): 732-741.

Olsen KW, Castillo-Fernandez J, Zedeler A, Freiesleben NC, Bungum M, Chan AC, et al. A distinctive epigenetic ageing profile in human granulosa cells. Hum Reprod. 2020; **35**(6): 1332-1345.

Park SU, Walsh L and Berkowitz KM. Mechanisms of ovarian aging. Reproduction. 2021; **162**(2): R19-R33.

Polyzos NP and Devroey P. A systematic review of randomized trials for the treatment of poor ovarian responders: is there any light at the end of the tunnel? Fertil Steril. 2011; **96**(5): 1058-1061 e1057.

Poseidon G, Alviggi C, Andersen CY, Buehler K, Conforti A, De Placido G, et al. A new more detailed stratification of low responders to ovarian stimulation: from a poor ovarian response to a low prognosis concept. Fertil Steril. 2016; **105**(6): 1452-1453.

Roque M, Valle M, Sampaio M and Geber S. Does freeze-all policy affect IVF outcome in poor ovarian responders? Ultrasound Obstet Gynecol. 2018; **52**(4): 530-534.

Seifer DB, Gardiner AC, Lambert-Messerlian G and Schneyer AL. Differential secretion of dimeric inhibin in cultured luteinized granulosa cells as a function of ovarian reserve. J Clin Endocrinol Metab. 1996; **81**(2): 736-739.

Shaw ND, Srouji SS, Welt CK, Cox KH, Fox JH, Adams JA, Sluss PM and Hall JE. Compensatory Increase in Ovarian Aromatase in Older Regularly Cycling Women. J Clin Endocrinol Metab. 2015; **100**(9): 3539-3547.

Skiadas CC, Duan S, Correll M, Rubio R, Karaca N, Ginsburg ES, Quackenbush J and Racowsky C. Ovarian reserve status in young women is associated with altered gene expression in membrana granulosa cells. Mol Hum Reprod. 2012; **18**(7): 362-371.

Sunkara SK, Khalaf Y, Maheshwari A, Seed P and Coomarasamy A. Association between response to ovarian stimulation and miscarriage following IVF: an analysis of 124 351 IVF pregnancies. Hum Reprod. 2014; **29**(6): 1218-1224.

Tatone C, Carbone MC, Falone S, Aimola P, Giardinelli A, Caserta D, et al. Age-dependent changes in the expression of superoxide dismutases and catalase are associated with ultrastructural modifications in human granulosa cells. Mol Hum Reprod. 2006; **12**(11): 655-660.

van der Stroom EM, Konig TE, van Dulmen-den Broeder E, Elzinga WS, van Montfrans JM, Haadsma ML and Lambalk CB. Early menopause in mothers of children with Down syndrome? Fertil Steril. 2011; **96**(4): 985-990.

Wang Y, Chen F, Ye L, Zirkin B and Chen H. Steroidogenesis in Leydig cells: effects of aging and environmental factors. Reproduction. 2017; **154**(4): R111-R122.

Zirkin BR and Chen H. Regulation of Leydig cell steroidogenic function during aging. Biol Reprod. 2000; **63**(4): 977-981.

Acknowledgments

I would like to thank Prof. Dr. Özgür Öktem for building and leading the Reproductive Medicine PhD program in Koç University and his full support throughout the program.

I would like to thank Dr. Gamze Bildik, Dr. Yashar Esmaelian and Dr. Francesco Hela for their sincere support during my education. None of these studies could have been accomplished without their help.

I gratefully acknowledge use of the services and facilities of the Koç University Research Center for Translational Medicine (KUTTAM), equally funded by the Republic of Turkey Ministry of Development Research Infrastructure Support Program.

Funding

Funded in part by the Koç University Seed Research Program Grant SF.00103, by the School of Medicine, the Graduate School of Health Sciences of Koc University and Koç University Research Center for Translational Medicine (KUTTAM), equally funded by the Republic of Turkey Ministry of Development Research Infrastructure Support Program and in part by the Scientific and Technological Research Council of Turkey Grant 109S164.